Acta Oceanol. Sin., 2023, Vol. 42, No. 11, P. 44–58
https://doi.org/10.1007/s13131-023-2191-9
http://www.aosocean.com
E-mail: ocean2@hyxb.org.cn

Sedimentary elements, evolutions and controlling factors of the Miocene channel system: a case study of the deep-water Taranaki Basin in New Zealand

Guangxu Wang[1], Wei Wu[1]*, Changsong Lin[2], Quan Li[1, 3], Xiaoming Zhao[4], Yongsheng Zhou[1], Weiqing Liu[1], Shiqin Liang[1]

[1] Institute of Resources and Environment, Henan Polytechnic University, Jiaozuo 454003, China

[2] School of Ocean Science, China University of Geoscience, Beijing 100083, China

[3] Institute of Exploration Technology, CNOOC International Ltd., Beijing 100028, China

[4] School of Geoscience and Technology, Southwest Petroleum University, Chengdu 610500, China

Received 10 December 2022; accepted 22 February 2023

Abstract

Deep-water channel systems are important petroleum reservoirs, and many have been discovered worldwide. Understanding deep-water channel sedimentary elements and evolution is helpful for deep-sea petroleum exploration and development. Based on high-resolution 3D seismic data, the Miocene channel system in the deep-water Taranaki Basin, New Zealand, was analyzed by using seismic interpretation techniques such as interlayer attribute extraction and strata slicing. The channel system was divided into five composite channels (CC-I to CC-V) according to four secondary level channel boundaries, and sedimentary elements such as channels, slump deposits, inner levees, mass transport deposits, and hemipelagic drape deposits were identified in the channel system. The morphological characteristics of several composite channels exhibited stark variances, and the overall morphology of the composite channels changed from relatively straight to highly sinuous to relatively straight. The evolution of the composite channels involved a gradual and repeated process of erosion and filling, and the composite channels could be divided into three evolutionary stages: initial erosion-filling, later erosion-filling (multistage), and channel abandonment. The middle Miocene channel system may have formed as a consequence of combined regional tectonic activity and global climatic change, and its intricate morphological alterations may have been influenced by the channel's ability to self-regulate and gravity flow properties. When studying the sedimentary evolution of a large-scale deep-water channel system in the Taranaki Basin during the Oligocene–Miocene, which transitioned from a passive margin to plate convergence, it can be understood how tectonic activity affected the channel and can also provide a theoretical reference for the evolution of the deep-water channels in areas with similar tectonic conversion environments around the world.

Key words: deep-water channel system, channel geomorphology, sedimentary evolution, climate and region tectonic activities, deep-water Taranaki Basin

Citation: Wang Guangxu, Wu Wei, Lin Changsong, Li Quan, Zhao Xiaoming, Zhou Yongsheng, Liu Weiqing, Liang Shiqin. 2023. Sedimentary elements, evolutions and controlling factors of the Miocene channel system: a case study of the deep-water Taranaki Basin in New Zealand. Acta Oceanologica Sinica, 42(11): 44–58, doi: 10.1007/s13131-023-2191-9

1 Introduction

With the continuous discovery of deep-water hydrocarbon resources, deep-water sedimentation has attracted increasing attention from the petroleum industry and sedimentology experts (Gee and Gawthorpe, 2006; Deptuck et al., 2007; Mayall et al., 2010; Wu et al., 2014; Steel et al., 2020; Rebesco et al., 2021). As an important deep-water hydrocarbon reservoir, the physical characteristics and distribution rules of channel sands can play an important role in guiding deep-water hydrocarbon exploration (Wu et al., 2018). Geologically, "deep water" refers mostly to regions outside the shelf break zone, such as the slope and the basin areas with water depths of more than 200 m. In marine engineering, "deep water" refers to the environment's present water depth, particularly to waters deeper than 500 m (Shanmugam, 2000). However, due to the data quality and complexity of the deep-water environment, the sedimentary elements and evolution process of the channels have been difficult to understand in the field of deep-water sedimentation (Babonneau et al., 2010; Li et al., 2019, 2020), so most sedimentary resolutions of deep-water channels were based on geophysical data. Some achievements have been made in the study of deep-water channel sedimentary evolution, Deptuck et al. (2007) divided channel evolution into two stages of erosion and filling by using high-resolution 3D seismic data and subdivided each stage into several periods. Babonneau et al. (2004) suggested that the evolution of a channel system was a gradual process.

The complexity of the deep-water channel evolution process leads to the diversity of channel architectures, and the internal architecture of a deep-water channel is so complex and highly heterogeneous that the porosity and permeability of the channel sand reservoir can change greatly within a short distance (Zhao et al., 2018a). Sedimentary elements such as slumps, lobes, chan-

Foundation item: The National Natural Science Foundation of China under contract Nos 42077410 and 41872112.
*Corresponding author, E-mail: wei@hpu.edu.cn

nels, and levees have different effects on the quality of hydrocarbon reservoirs. Prather (2003) suggested that slumps with heavily deformed internal architecture severely affect the mobility and storage capacity of a channel reservoir and generally do not act as hydrocarbon reservoirs. Li et al. (2019) proposed that the terminal lobe has the characteristics of good continuity and well-developed pores and can be used as an important hydrocarbon reservoir. In the process of global hydrocarbon exploration and development, the sand content of filling sediment in deep-water channels is very high, and it has become an important target of deep-water hydrocarbon exploration due to its large scale, superior reservoirs, and high production (Mayall et al., 2006; Wynn et al., 2007; Qin et al., 2016). A levee sand body is an important type of hydrocarbon reservoir with high internal connectivity, but it also presents a major problem in the process of hydrocarbon development due to the thin thickness of the sand body (Li et al., 2013). Therefore, the identification of deep-water channel sedimentary elements and the study of petroleum reservoir potential are of great significance for the exploration and development of deep-sea petroleum resources (Li et al., 2021), which can provide a reference for subsequent well location design and drilling and reduce drilling risk (Zhao et al., 2018a).

There are many control factors in the complex evolutionary processes of channels. The submarine topography is the primary factor controlling the morphology and migration of the channels (Mayall et al., 2010; Gamboa and Alves, 2015), and the underlying rock properties and bottom current can also directly affect the sedimentation characteristics of the channels (Abreu et al., 2003; Gee and Gawthorpe, 2006; Gong et al., 2013; Zucker et al., 2017; Wu et al., 2018; Li et al., 2020; Fonnesu et al., 2020). For instance, the accretion and consolidation of levees can limit the change in the channel morphology to a certain extent (Gee and Gawthorpe, 2006; Deptuck et al., 2007), making the channel difficult to bend. Global sea-level fluctuations, tectonic activities, and other factors can also influence channel development (Kolla et al., 2007).

The offshore area of the Taranaki Basin in New Zealand is a world-class mass transport deposits (MTDs) and channel research example area (Li et al., 2017; Nwoko et al., 2020), and a large-scale Miocene deep-water channel sedimentary system has developed (Wang et al., 2022). Bull et al. (2019) analyzed Miocene sediments in the southern Taranaki Basin, New Zealand, using a multidisciplinary approach and proposed that the formation of the New Zealand plate boundary was closely related to the increase in sediment input in the Miocene Taranaki Basin. In addition, the sedimentary mechanism and evolution of the Miocene sediment in the petroleum reservoirs in the southern Taranaki Basin were related to the formation of the New Zealand plate boundary, the uplift of the hinterland of the South Island and the increase in clastic sediment input (King and Thrasher, 1996; Baur, 2012; Higgs and King, 2018; Bull et al., 2019).

Previous studies have found different types of deep-water channels in different continental margin basins around the world and discussed their evolutions and controlling factors (Deptuck et al., 2007; Li et al., 2019). However, these channels vary greatly in their evolution under different geological backgrounds and tectonic conditions, which has attracted the attention of relevant researchers around the world. The Taranaki Basin changed from a passive continental margin to plate convergence during the Oligocene–Miocene, and tectonic activities, and sea-level fluctuations played different leading roles in different stages of the channel system. In this context, this study systematically analyzes the sedimentary evolution of the channel system formed by multiphase gravity flow activity and its corresponding control factors. Particular questions that are addressed as follows. (1) How can the sedimentary elements within the channel system be identified? (2) Compared with the evolution of the channels in other areas, how does the channel system in this study area evolve and what are the differences? (3) What are the major controlling factors of the sedimentary evolution process of the channel system? The results of this study could provide a reference for channel evolution research in similar deep-water sedimentary environments in the region and even the world, and could enrich the theory of deep-water deposition and provide different research ideas for other researchers around the world.

2 Geological setting

2.1 *Regional setting*

The study area (Romney 3D survey) covers an area of ca. 1 925 km^2 of the deep-water Taranaki Basin, which has a total area of ca. 330 000 km^2 (Panpichityota et al., 2018). Taranaki Basin in New Zealand is located in the offshore area of western New Zealand. It is one of several large sedimentary basins formed by the rupture of the ancient Pacific rim of Gondwana in the Late Cretaceous (Muir et al., 2000). The Taranaki Basin is bounded by the Taranaki Fault (TF) on the eastern side, which marks a convergent boundary between the Australian and Pacific Plates (King and Thrasher, 1992). Deep-water Taranaki Basin is located in deep water area on the northwest side of the Taranaki Basin and is surrounded by tectonic units such as Northland Basin (NB), West Norfolk Ridge (WNR), New Caledonia Trough (NCT), Lord Howe Rise (LHR) and Challenger Plateau (CP) (Fig. 1a) (King and Thrasher, 1996). The three-dimensional seismic data in the study area cover an area of about 1 700 km^2 with a water depth of more than 1 000 m. The overall exploration degree of the basin was low (Higgs et al., 2010), and a large channel system was identified in the Miocene strata (Figs 1b and c).

2.2 *Tectonic evolution characteristics*

The deep-water Taranaki basin in New Zealand can identify continental sedimentary strata different from those in shallow water and land, indicating that the deep-water area of the Taranaki Basin had undergone a tectonic evolution process different from those inland and shallow water (Collot et al., 2009; Uruski, 2010) (Fig. 1d).

At the end of the Oligocene, due to the rise of sea level, the northwest sea area of New Zealand reached the maximum flooding period (King and Thrasher, 1996; Strogen et al., 2014). Since the Miocene, the formation of the modern plate boundary in New Zealand had provided a large amount of provenance from the southeast for the Taranaki Basin (King, 2000; Uruski and Warburton, 2015; Bull et al., 2019; La Marca and Bedle, 2022). At the same time, affected by the evolution of the Australian-Pacific plate transition boundary (Alpine fault), the supply of terrigenous clastic sediment in the Middle-Miocene basin also gradually increased (Bull et al., 2019), and the continental shelf margin expanded westward (King and Thrasher, 1992), ending the previous rising sea-level change trend and the regression sequence began. The Miocene regressive sequence was characterized by fine-grained clastic deposits and developed slope fan and basin floor fan (Baur, 2012; La Marca and Bedle, 2022). In the middle-late Miocene, volcanic eruptions occurred in the northern part of the basin, forming volcanoclastic deposits. The late Miocene Pliocene basin floor fan overlapped the volcanic complex. In addition, during the Late Miocene–Quaternary period, multiple large-scale mass transport deposits (MTDs) were also developed in the Taranaki Basin (Nwoko et al., 2020).

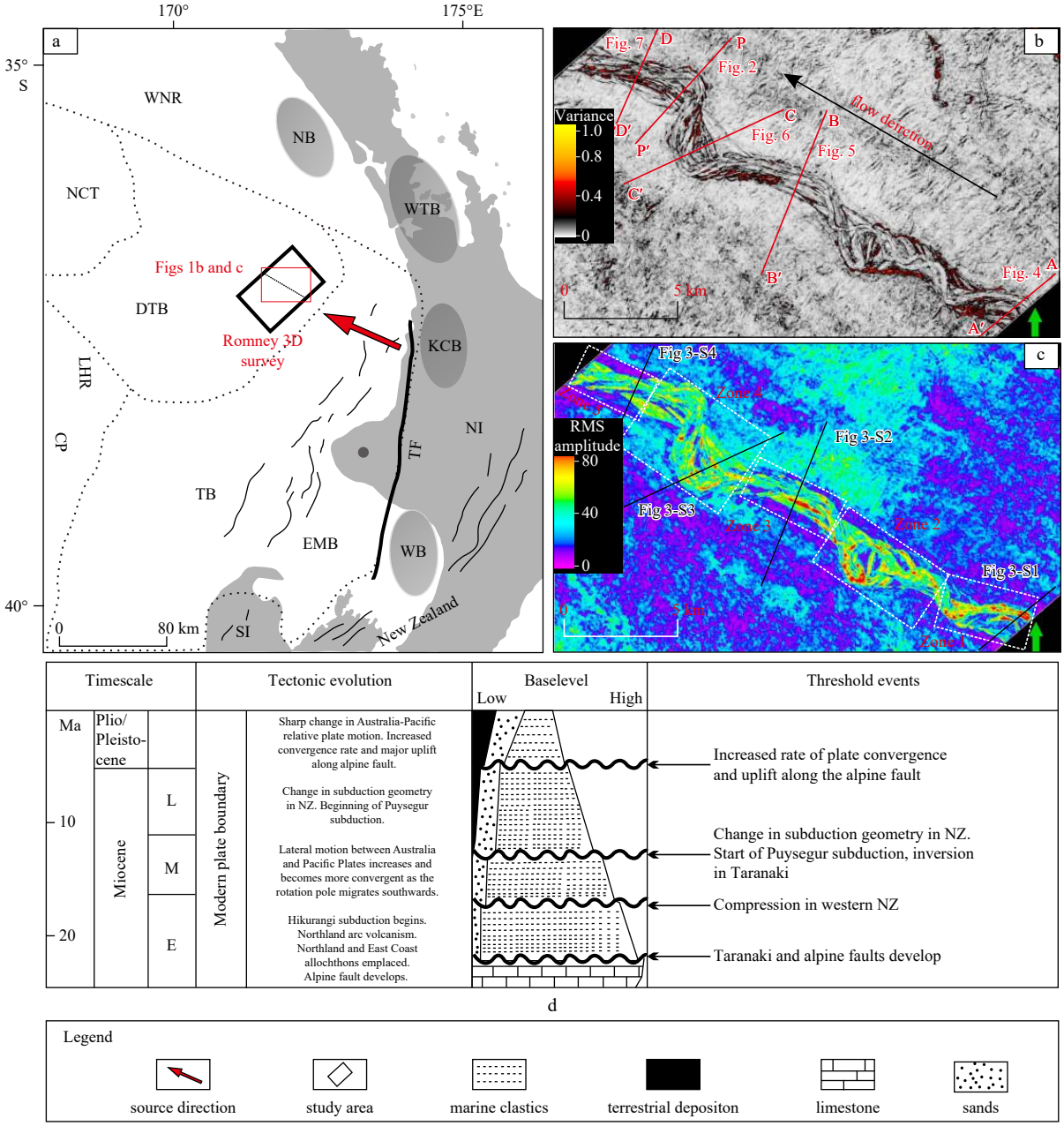

Fig. 1. Geographical location map of the study area (Romney 3D survey) (a); map of the variance attribute of the channel system (b); map of the root-mean-square (RMS) amplitude attribute of the channel system (c); tectonic evolution history of the New Zealand Basin in the Miocene (modified after Uruski, 2010) (d). The black box in a represents the location of the study area, the red box in a represents the location of the target channel, the red arrow in a represents the direction of the source, and the black line segment in a represents the fault. The abbreviation in a are showed in Table 1.

3 Methodology and data

3.1 *Seismic data for characterizing sedimentary records*

The 3D seismic exploration data of this study were obtained by the Anadarko Company of New Zealand from October 23 to December 6, 2011, and processed by the ION Geophysical Company in February 2013 (NZP and M oil reports can be obtained from www.nzpam.govt.nz). The vertical sampling interval of the 3D seismic data volume is 4 ms (TWT: two-way travel time), and the bin space is 25 m × 25 m. The main frequency is nearly 35 Hz, and the interval velocity is approximately 1 850 m/s, so the vertical resolution is approximately 13 m, which can meet the needs of this study (Li et al., 2017). In addition, due to the abbreviations used in this paper, all the abbreviations are summarized in the table to better facilitate reading (Table 1).

Identification and mapping of ancient and modern submarine channel systems were successfully obtained by using a 3D seismic geomorphological approach (Posamentier, 2003; Kolla et al., 2007; Zhao et al., 2018b). This study was based on high-resolution 3D seismic data, and the geological information contained in the seismic data can provide data support for deep-water channel research. Seismic facies represent different sedimentary elements of sedimentary records, and they are recognized and defined mainly by their external geometry internal reflection

Table 1. Summary of the abbreviations of the main nouns in the paper

Abbreviation	Full name	Abbreviation	Full name
CC	complex channel	LMC	lateral migration channel
SC	single channel	VS	RSC-vertical sand-rich stack channel
TF	Taranaki fault	VM	RAC-vertical mud-rich aggradation channel
WNR	West Norfolk Ridge	SEC	single erosion channel
NCT	New Caledonian Trough	SAC	single aggradation channel
NB	Northland Basin	SDs	slump deposits
LHR	Lord Howe Rise	IL	inner levee
CP	Challenger Plateau	MTDs	mass transport deposits
TB	Taranaki Basin	HDDs	hemipelagic drapes deposits
SI	South Island	RC	remnant channel
NI	North Island	RMS	root mean square
DTB	deep-water Taranaki Basin	TWT	two-way travel time
KCB	King Country Basin	FLCB	first level channel boundary
WB	Wanganui Basin	SLCB	secondary level channel boundary
EMB	Eastern Mobile Belt	TLCB	third level channel boundary

structure, amplitude, continuity, and strata terminations (Qi et al., 2022).

In addition, the difference in the channel filling deposition properties can produce a high wave impedance difference, thus forming an obvious seismic reflection interface (i.e., channel erosion interface) in the seismic profiles. According to the different levels of the channel erosion interface, the development period of the channel system can be identified, and the sedimentary evolution process of the channel system can be understood.

3.2 *Seismic attributes for characterizing channel morphology and sediment properties*

Seismic interpretation software was used to track and interpret the top and bottom interfaces of the target interval; 9 strata slicings were generated by uniform interpolation in equal proportion between the top and bottom interfaces, and seismic attributes [root mean square (RMS) amplitude and variance] were extracted along the slice. The amplitude attribute can reflect the properties of the channel-filling sediments. Generally, strong amplitude reflections represent sand-prone sediments, and weak amplitude reflections represent mud-prone sediments (Xie and Deng, 2013; Chima et al., 2019; La Marca Molina et al., 2020). The variance attribute can delineate the boundary of the sedimentary body by calculating the similarity between adjacent seismic tracks, which plays an important role in analyzing the plane distribution of the channels (La Marca Molina et al., 2020) (Fig. 1b). The combination of seismic profile analysis, interlayer attribute extraction, and strata slicing is helpful to the study of sedimentary characteristics and evolution process of the deep-water channel.

4 Results

In the deep-water area of the Taranaki Basin, New Zealand, a large channel system was identified in the Miocene strata (Figs 1b and c). According to the plane morphological characteristics of the channel system and the distance from the source area, combined with the RMS amplitude attribute strata slicing, the channel system was divided into five zones, namely, the near-source zone (Zone 1), the complex change zone of the channel path (Zone 2), the straight morphology zone (Zone 3), the high sinuous morphology zone (Zone 4) and the far source zone (Zone 5). Typical seismic profiles of the different zones were chosen, and channel erosion interfaces with clear characteristics on the seismic profiles could be detected, based on which the development stage of each composite channel in the channel system could be distinguished.

4.1 *Identification of the channel boundary and its development stage*

4.1.1 *Level division of the channel boundary*

Deep-water channels can be subdivided into single channels, composite channels, composite channel sets, and channel systems (Alpak et al., 2013). According to the seismic reflection termination relationship and magnitude, three levels of the channel boundary were identified in the seismic profiles (Fig. 2b). Based on this, it was determined that the deep-water channel in the study area was a channel system formed by the mutual erosion and superposition of multiple composite channels (Fig. 2c).

The first level channel boundary (FLCB) was the interface between the channel system and the surrounding rock. Two interfaces (FLCB-1–2) were identified in the seismic profiles. FLCB-1 had a concave erosion shape, good continuity, and strong wave impedance difference. Channel deposits were filled above FLCB-1, whose seismic reflection characteristics, such as the amplitude and continuity of channel sediments, were significantly different at different positions. Under FLCB-1, there was a normal sedimentary stratum, which presented layered and continuous seismic reflection characteristics. FLCB-2, whose seismic reflection was characterized by strong amplitude and high continuity, was an overlapping interface located at the top of the channel system, and its distribution range was beyond the underlying channel system.

The secondary level channel boundary (SLCB) was the local erosion interface between composite channels, and four interfaces (SLCB-1–4) were identified (Fig. 2b). This type of interface was generally small in scale and presented a concave erosion shape, which was often damaged by the later channels, resulting in incomplete interface morphology. The top of SLCB-1 was truncated, and different channel-filling deposits developed on the left and right sides. The first type of channel deposition showed seismic reflection characteristics with a strong amplitude and good continuity at the bottom and weak amplitude and disorderly reflection in the upper part. Another channel deposition was characterized by imbrications, strong amplitudes, and intermittencies on the bottom, which was similar to the lateral accretion package (LAP) characteristics proposed by Abreu et al. (2003). This could be explained as the bottom lateral migration channel,

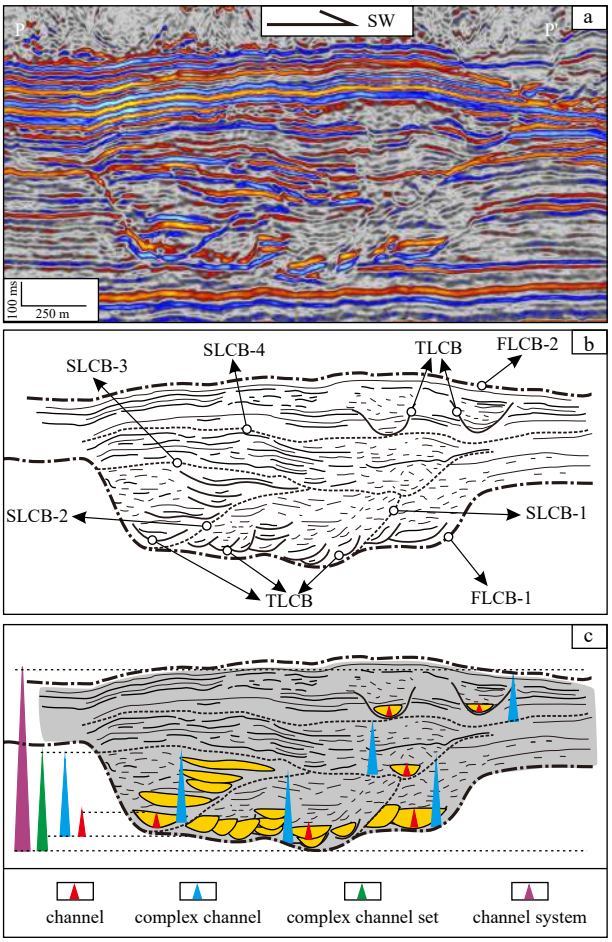

Fig. 2. Classification of deep-water channel and identification of the channel boundary. Original seismic profile, the location of the seismic profile is shown in Fig. 1b (a); seismic profile interpretation (b); schematic diagram of classification of the deep-water channel (c). The yellow part in the schematic diagram represents strong amplitude reflection deposits, which can generally be interpreted as channel sand-rich deposits.

while the upper part of the channel deposition was characterized by weak amplitude and disorderly reflection. SLCB-2 showed a "U" or "V" shape on the seismic profiles. The sedimentary characteristics of the channels on both sides were quite different. One type was the lateral migration channel. On the other hand, in the relatively straight morphology, another channel deposition was vertically superimposed, showing parallel or subparallel characteristics, strong amplitude, and high continuity seismic reflection. In the high sinuous morphology, the channel deposition was vertically superimposed and offset, showing parallel or subparallel seismic reflection characteristics, strong amplitude, high continuity, and coexistence with medium-weak amplitude and poor continuity. SLCB-3 had a large scale and good continuity, covering almost the whole channel system. Two types of channel deposition developed above the interface, and one type was characterized by medium-weak amplitude, poor continuity, and disordered reflection, which were similar to the characteristics of mass transport deposits (MTDs) explained by Li et al. (2019). The other was parallel or subparallel, with medium-strong amplitude, and good continuity. The scale of SLCB-4 was the largest. Some positions of this interface had exceeded the scope of early sedimentary accommodation. Multiple erosion single channels were developed above the interface. However, the internal filling and reflection characteristics of the single channel could not be identified.

The third level channel boundary (TLCB) was the erosion surface between single channels. This type of interface was small in scale but large in number and was not easy to be identify in the seismic profiles. It was difficult to retain the complete shape due to the erosion of later channels (Fig. 2b).

4.1.2 *Division of the development stages of the channel system*

According to the four secondary level channel boundaries, the channel system was divided into five stages of the composite channel (CC-Ⅰ-Ⅴ) (Fig. 3c). The CC-Ⅰ was characterized by remnant channel architecture, and the scale of the remnant channel architecture was a difference in different regions. The CC-Ⅱ was characterized by lateral migration, and the migration distance was the largest in Zone 4. The CC-Ⅲ was characterized by vertical superimposition. The thickness of the channel deposition was large. In Zone 3, the vertical superimposition was a major characteristic, while in Zone 4, the vertical superimposition of the channel was accompanied by a small-scale lateral migration. The distribution range of the CC-Ⅳ was large, which could almost cover the whole sedimentary accommodation. The CC-Ⅴ was characterized by the disorderly distribution of single channels, the development position of numerous channels was not restricted within the spatial distribution of the previous composite channel.

Constrained by the strata slicing, the width and depth of the channel system were measured by four typical seismic profiles (Fig. 3c), and indirectly reflect the plane morphology of the channel system (Figs 3a and b). The depth of the channel system varied slightly, with a maximum depth of about 367.93 m, a minimum depth of about 324.47 m, and an average depth of about 339.8 m (Fig. 3c). The channel width in Zone 1 was about 2 969.35 m, that in Zone 3 was reduced to about 1 396.34 m, that in Zone 4 was increased to about 4 245.98 m, and that in Zone 5 was reduced to about 1 566.45 m (Fig. 3c).

4.2 *Sedimentary elements of the channel system and its seismic facies characteristics*

The use of seismic data to identify channel internal sedimentary elements was significantly more common in the process of previous research and actual exploration, and the seismic reflection characteristics of numerous sedimentary elements were summarized (external morphology, internal structure, continuity, amplitude, etc.). The outer levee, for instance, exhibits medium-weak amplitude, high continuity, and wedge-like seismic reflection features, whereas mass transport deposits exhibit variable amplitude, and discontinuous, chaotic, or blank seismic reflection characteristics. By identifying the seismic facies, the sedimentary properties of the internal structure of the channel can be known in advance, providing data support for the subsequent forecast of the distribution of the channel sand reservoir.

Therefore, this paper analyzes the typical seismic profiles of various zones, along with the seismic facies characteristics and previous research findings, and identifies five different types of channel sedimentary elements, including channels, slump deposits, inner levees, mass transport deposits, and hemipelagic drape deposits. Among them, although slump belongs to the category of mass transport deposits (MTDs), there are differences between them. Moscardelli and Wood (2008) believed that MTDs could be divided into three types according to source location: shelf-attached systems, slope-attached systems, and locally de-

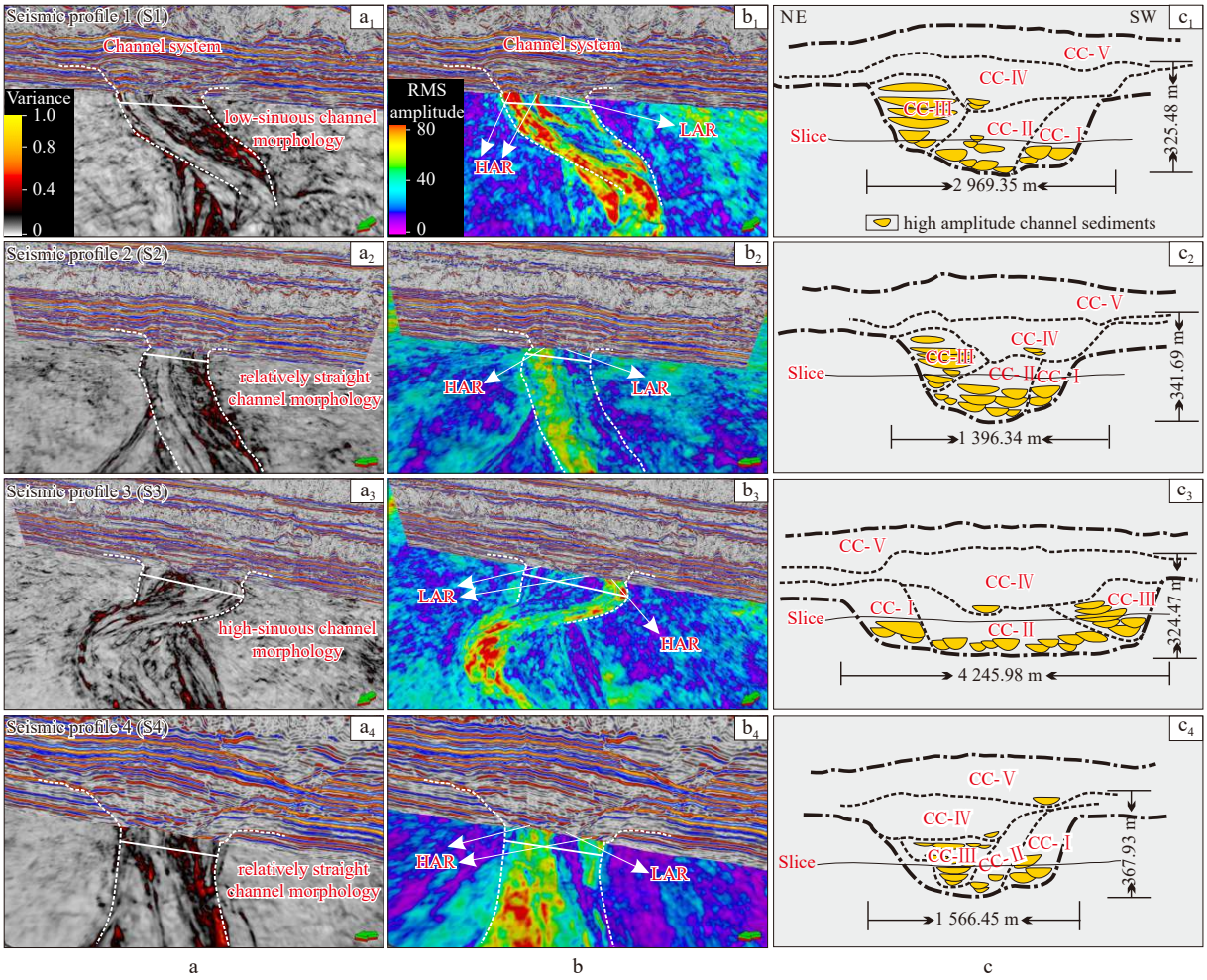

Fig. 3. Joint display of seismic profiles (Seismic profile 1–4: S1–S4) and strata slicings of different attributes of the channel system (the location of the seismic profiles is shown in Fig. 1c), and distribution characteristics of the channel sand bodies in each composite channel. HAR: high amplitude reflection; LAR: low amplitude reflection.

tached systems. The mass transport deposits of shelf-attached systems and slope-attached systems were supplied by the shelf-edge deltas and the upper slope, respectively, which have the characteristics of a large scale and wide distribution range. The source of the locally detached systems was a submarine volcano and the channel sidewalls, which have the characteristics of small scale and local distribution. Therefore, in this study, we believe that when dividing the sedimentary units in the deep-water channel system, the mass transport deposits of different source locations can be named separately. The sedimentary body formed by collapse due to the instability of the channel sidewall was deemed a slump, and the large-scale chaotic filling sediment formed from large-scale sources such as the shelf-slope areas in the channel system was deemed mass transport deposits (MTDs). At the same time, through the study of field outcrops, scholars have also found that slumps were the most common component in the turbidite channels (Clark and Pickering, 1996; Eschard et al., 2003; Mayall et al., 2006).

4.2.1 *Channels*

Channels were the most recognizable sedimentary element and had the characteristics of undercut filling seismic facies. Remnant channels (RC), lateral migration channels (LMC), vertical sand-rich stack channels (VS-RSC), vertical mud-rich aggradation channels (VM-RAC), single erosion channels (SEC), and single aggradation channels (SAC) were identified in the channel system (Figs 4–7). Among these, the bottom of the first three channels (RC, LMC, and VS-RSC) can be occupied by sediments with a strong amplitude, which has the potential to create hydrocarbon reservoirs.

(1) The bottom of the RC showed parallel or sub-parallel, strong amplitude, and high continuity seismic reflection characteristics, and the middle and upper part was characterized by weak amplitude and medium-poor continuity seismic reflection (Fig. 4g).

(2) The LMC showed imbrication, strong amplitude, and discontinuous seismic reflection characteristics in the seismic profiles (Fig. 5g). The lateral migration distance of the LMCs in different regions was quite different, which indirectly reflected the sinuous degree of the channel (Figs 6a, b and h).

(3) The VS-RSC presented parallel or subparallel, strong amplitude, and high continuity seismic reflection characteristics, and showed a “U” shape profile (Fig. 5g). There were differences in the movement modes of VS-RSC in different regions. The channels in Zone 4 were mainly vertically superimposed accompanied by lateral migration (Figs 6a, b, and h), while in the low sinuous or relatively straight shape regions, they were mainly vertically superimposed (Figs 5a, b, and h).

(4) In the VM-RAC, a “binary structure” was observed. Filling sedimentation at the bottom of the channel was characterized by

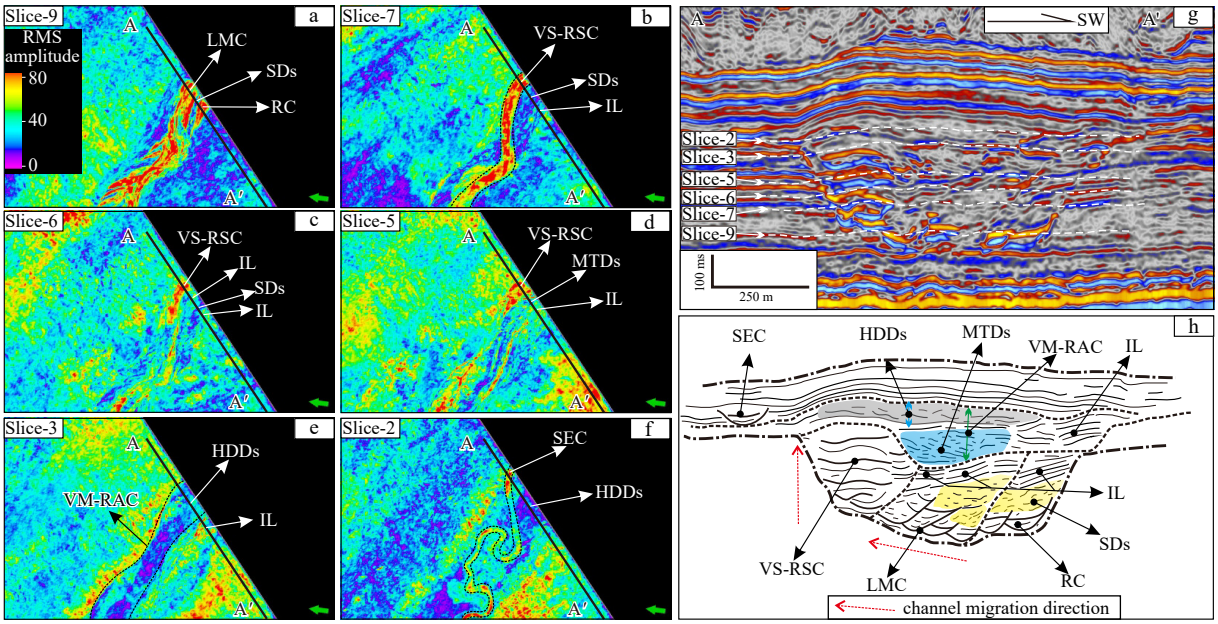

Fig. 4. Typical seismic profile and RMS attribute-extraction maps of the channel system in Zone 1. a–f. RMS amplitude attribute strata slicing. Red and yellow represent strong amplitude deposition, mostly sand facies sediments, and blue and green represent weak amplitude deposition, mostly mud facies sediments. g. Typical seismic profile in Zone 1. The white dotted line indicates the strata slicing position. h. Interpretation diagram of the typical seismic profile, where the red dashed arrow indicates the direction of movement of the channel.

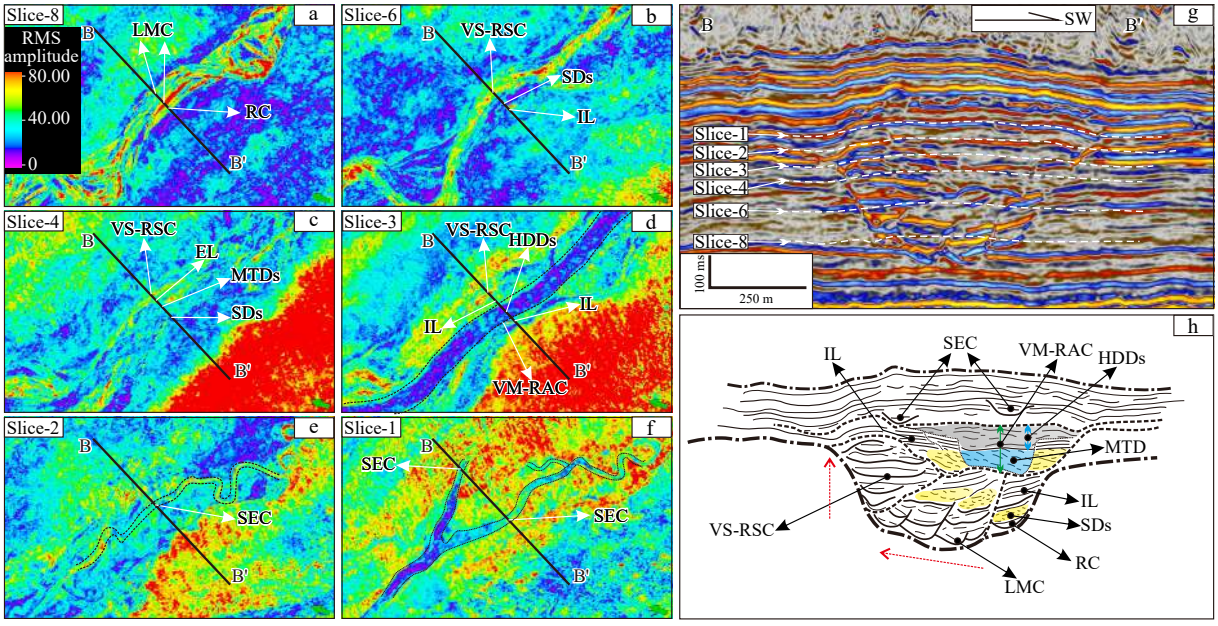

Fig. 5. Typical seismic profile and RMS attribute-extraction maps of the channel system in Zone 3. a–f. RMS amplitude attribute strata slicing. Red and yellow represent strong amplitude deposition, mostly sand facies sediments, and blue and green represent weak amplitude deposition, mostly mud facies sediments. g. Typical seismic profile in Zone 1. The white dotted line indicates the strata slicing position. h. Interpretation diagram of the typical seismic profile, where the red dashed arrow indicates the direction of movement of the channel.

weak amplitude, chaos, and no obvious geometric shape of seismic reflection. Filling sedimentation at the top was characterized by weak amplitude, low continuity, chaos, or blank reflection (Figs 5g and h). The VM-RAC was generally in the form of "narrow at the bottom and wide at the top". An obvious erosion interface was identified in the lower part, while the upper part was characterized by wide distribution and large thickness.

(5) Due to the limitation of the seismic resolution, it was difficult to observe the seismic characteristics of the internal architecture of the SEC, and only the overall "V" shape profile could be identified (Figs 5g and h). Several SECs converged downstream of the channel system to form the large-scale SAC (Figs 7f and h). The lower sediment was characterized by parallel or subparallel, medium-strong amplitude, and medium-high continuity seismic

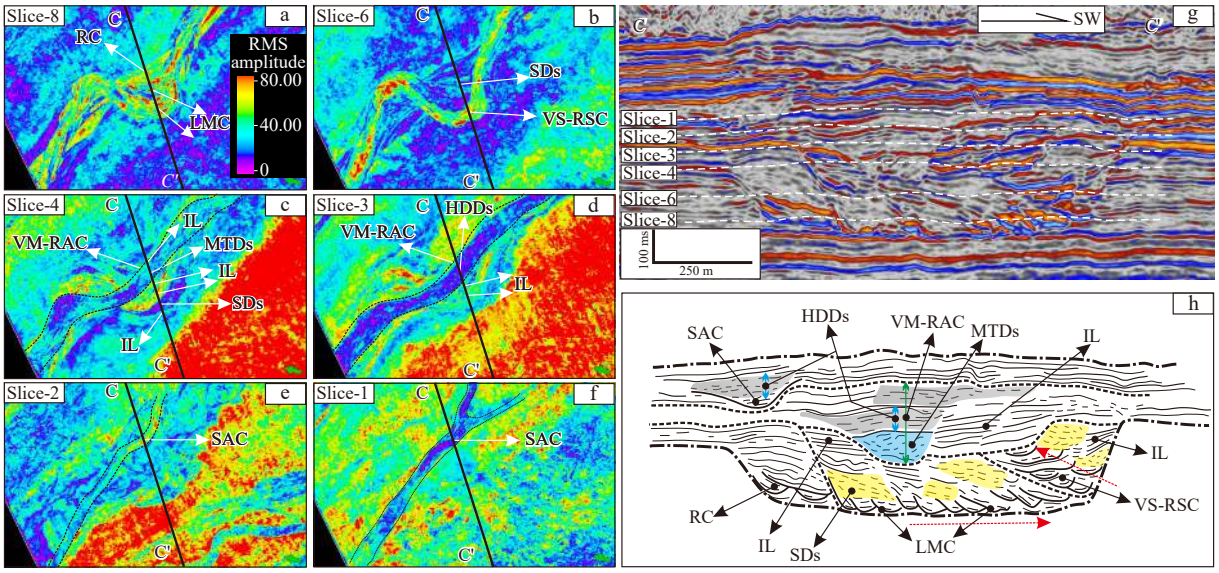

Fig. 6. Typical seismic profile and RMS attribute-extraction maps of the channel system in Zone 4. a–f. RMS amplitude attribute strata slicing. Red and yellow represent strong amplitude deposition, mostly sand facies sediments, and blue and green represent weak amplitude deposition, mostly mud facies sediments. g. Typical seismic profile in Zone 1. The white dotted line indicates the strata slicing position. h. Interpretation diagram of the typical seismic profile, where the red dashed arrow indicates the direction of movement of the channel.

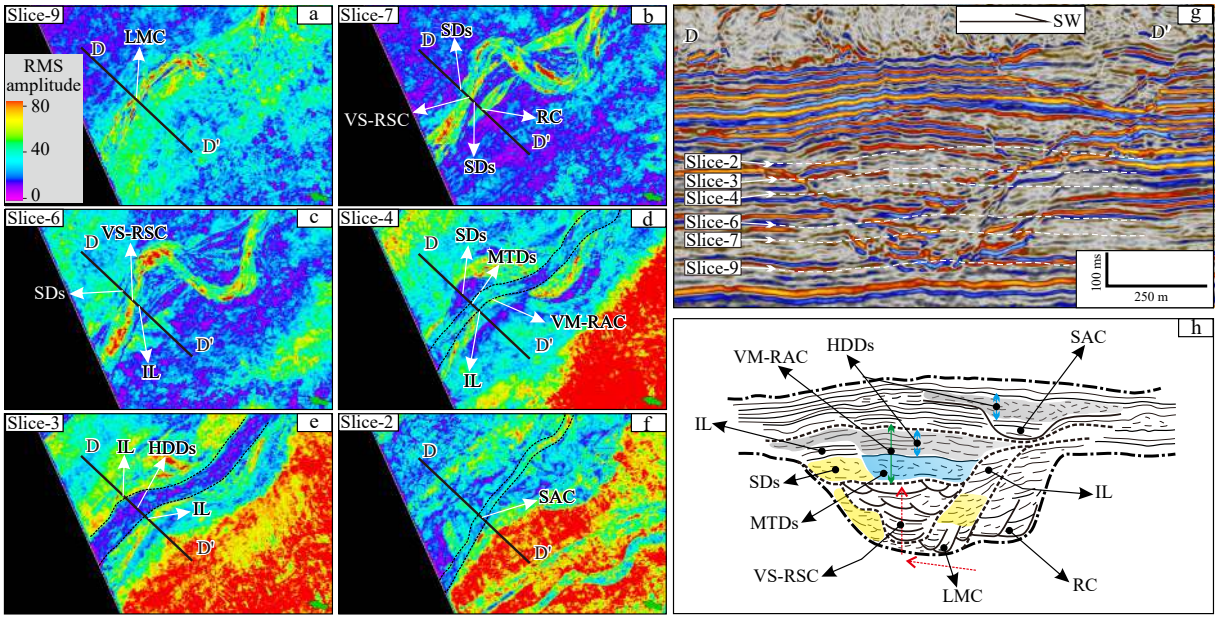

Fig. 7. Typical seismic profile and RMS attribute-extraction maps of the channel system in Zone 5. a–f. RMS amplitude attribute strata slicing. Red and yellow represent strong amplitude deposition, mostly sand facies sediments, and blue and green represent weak amplitude deposition, mostly mud facies sediments. g. Typical seismic profile in Zone 1. The white dotted line indicates the strata slicing position. h. Interpretation diagram of the typical seismic profile, where the red dashed arrow indicates the direction of movement of the channel.

reflection, while the upper sediment was characterized by medium-weak amplitude and poor continuity seismic reflection (Fig. 7g).

4.2.2 *Slump deposits (SDs)*

The consolidation degree of the sediment on the sidewall of the channel was weakened due to fluid scouring, which led to collapse and accumulation at the bottom of the channel, forming slump deposits, which were mostly characterized by weak amplitude, discontinuity, and chaotic seismic reflection (Figs 4g and 6g) and were highly developed in the channel system (Figs 4h and 6h). Generally, this architecture has poor internal connectivity and cannot be used as a favorable hydrocarbon reservoir.

4.2.3 *Inner Levees (ILs)*

Levee deposits can be divided into outer levees and inner

levees according to their development position. The inner levee deposits in the target channel system (Figs 4–7), which were mostly formed by the stable accumulation of sediment, with parallel, weak-amplitude, and high-continuity seismic characteristics, and were mostly developed above the slump deposits (Fig. 4h). The inner levee mostly develops at the margin of the channel, and the internal sediment particles are generally fine, so it is difficult for it to become a good hydrocarbon reservoir.

4.2.4 *Mass transport deposits (MTDs)*

The MTDs in the target channel system were characterized by medium-weak amplitude, poor continuity, and chaotic reflection (Figs 6g and 7g). MTDs had strong cutting erosion ability in the early stage of channel development and could form obvious erosion surfaces with surrounding rock (Figs 6h and 7h). The strong amplitude sediment was identified at the bottom of the MTDs and gradually change upward to weak amplitude sediment. MTDs have strong internal heterogeneity and basically can not be used as a good hydrocarbon reservoir, but it can be used as a high-quality regional cap rock. Moreover, there were differences between MTDs and slump deposits, the distribution of the MTDs range was larger than the slump deposits, and at the same time, the MTDs showed different seismic reflection characteristics due to the difference in provenance properties, the MTDs formed by sand-rich source was mostly characterized by strong amplitude, discontinuity, and chaotic reflection, while the MTDs formed by mud-rich source were similar to the slump deposits formed by the collapse of the channel side walls, showing the reflection characteristics of weak amplitude, discontinuity, chaotic or blank.

4.2.5 *Hemipelagic drape deposits (HDDs)*

The HDDs were mostly developed under the condition of hydrodynamic stability, which marked the abandonment of the deep-water channels. In seismic profiles, they were characterized by weak amplitude, low continuity, chaos, or blank seismic reflection (Figs 4g and 7g). Because of the low porosity and low permeability of the HDDs, it played a good capping role and could be used as the regional caprocks of hydrocarbon resources (Figs 4h and 7h).

4.3 *Sedimentary elements stack characteristics of different composite channels*

The internal architecture of the channel system was complex, and a variety of channel sedimentary elements had been identified. By using the seismic profile, the stacked relationship of different sedimentary elements in each composite channel was disentangled.

The bottom of the CC-Ⅰ was mostly filled with strong amplitude sediment, and there was multi-stage single-channel lateral stacking in some areas. On top of the strong amplitude deposits at the bottom of the channel, slump and inner levee deposits with weak amplitude reflection were developed (Fig. 4h), while the HDDs were mostly developed at the top of the CC-Ⅰ.

At the bottom of the CC-Ⅱ, there were imbricated, strong amplitude and discontinuous channel axial filling deposits, which have a lateral stacking relationship in space. Many SDs formed by the instability of the side wall of the channel were developed above the strong amplitude deposits of the bottom lateral migration channel. In a stable environment after slump deposits, the inner levee deposits with weak amplitude and good continuity were developed on this basis.

The CC-Ⅲ, in Zone 1, Zone 3, and Zone 5, the channels were dominated by vertical superimposing, and their interior space was filled with strong amplitude sediment (Fig. 5h), which could be interpreted as the VS-RSC. Meanwhile, the HDDs were developed at the top of the channels. In Zone 4, the channels were mainly vertically superimposed accompanied by lateral migration. The channels were also filled with strong amplitude deposits, but weak amplitude slump and inner levee deposits were developed at the edge of the channel.

The internal filling sedimentation of the CC-Ⅳ was characterized by "segmentation". The lower part was developed with MTDs, with obvious undercut erosion morphology on the seismic profiles. The upper part was developed with the HDDs with a wide distribution range and large deposition thickness (Fig. 7h), which could be interpreted as the VM-RAC.

The CC-V was composed of multiple single channels, each of which was isolated in space and has a concave erosion shape on the seismic profile, which could be interpreted as the SEC. Several SECs converged downstream of the channel system to form the SAC. The bottom of the channel developed deposits with medium-strong amplitude and good continuity, while the upper part developed the HDDs with weak amplitude.

5 Discussion

5.1 *Morphology and migration characteristics of the channel system*

The original morphology of CC-Ⅰ was obtained according to the boundary of the remnant channel deposition and the overall movement trend (Figs 8a and 9a). The channel as a whole shows a relatively straight morphology, with a small bend at the distal position, and the overall width of the channel changes little, but the channel width of the distal area is larger than that of the proximal area (Fig. 9a).

Five single channels were identified in CC-Ⅱ (Fig. 8b). The movement trajectories of single channels 1, 2, and 3 were roughly the same, but there were migration movements between single channels at different stages. Two types of channel migration were identified, namely, downstream migration and lateral migration (Fig. 9) (Wang et al., 2022). The migration of the single channel may be affected by the changes in the size and energy strength of the fluid in the channel. Compared with the single channel in the previous three stages, the sinuosities of the single channels 4 and 5 gradually increased. On the other hand, the sinuosity of CC-Ⅱ increased rapidly in Zone 2, but the change was not regular (Fig. 8b), and the lateral migration movement of the channel in Zone 4 also continued to develop.

Two single channels were identified in CC-Ⅲ. The plane morphology of single channel 1 was relatively straight in the middle to upper reaches (Zones 1, 2, and 3) and highly sinuous in the lower reaches (Zones 4 and 5). The motion path of single channel 2 was inherited from single channel 1, but its overall width gradually increased (Fig. 8d). However, the sinuosity of CC-Ⅲ was significantly reduced compared with the corresponding segment of CC-Ⅱ (Fig. 9c).

Combined with the seismic profiles, it was speculated that there were two stages of single channels in CC-Ⅳ. Affected by the early stages of CC-Ⅱ and CC-Ⅲ, CC-Ⅳ inherited the negative topographic characteristics of the early channels. The distribution range of single channel 1 was large, but the specific plane morphology was difficult to identify (Fig. 8e). Single channel 2 was in a relatively straight plane morphology due to the cutting erosion of the mass transport deposition and the filling of the hemipelagic drape deposits (Figs 8g and 9d).

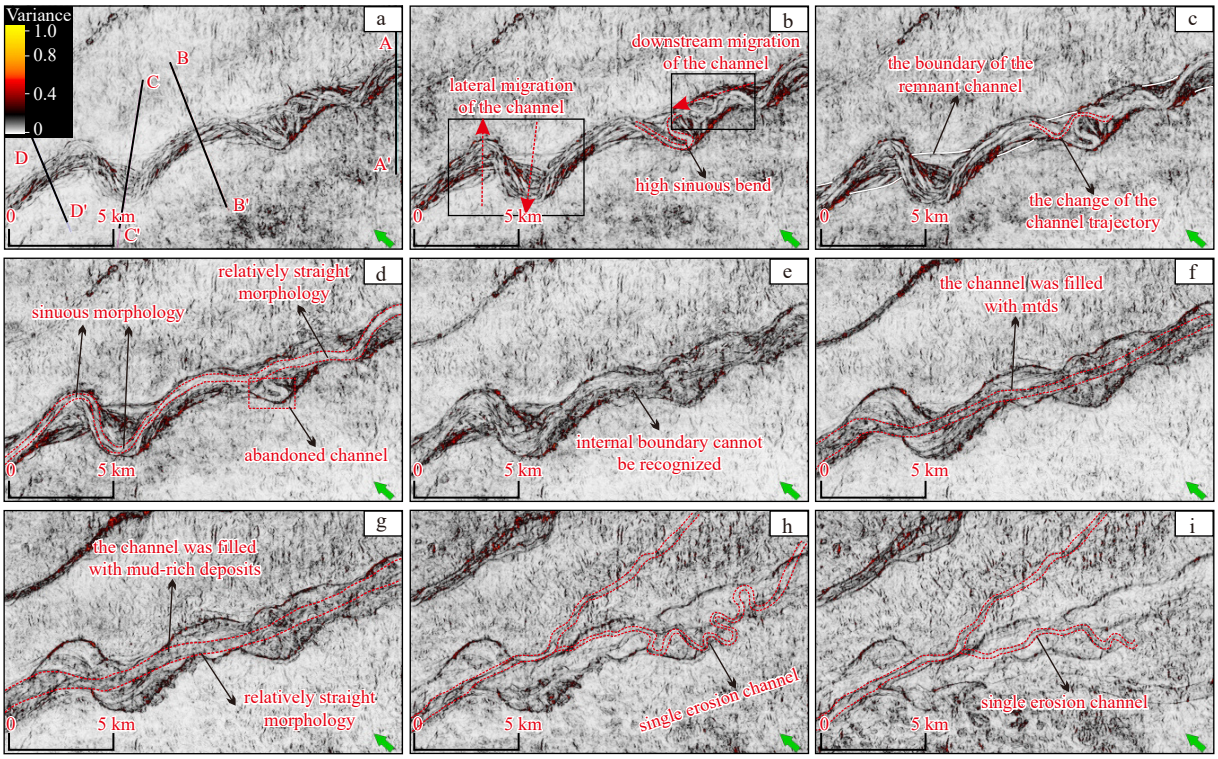

Fig. 8. Variance attribute-extraction maps of the channel system. The red dashed lines represent the morphology of different channels, and the red dashed arrows indicate the migration direction of the channels.

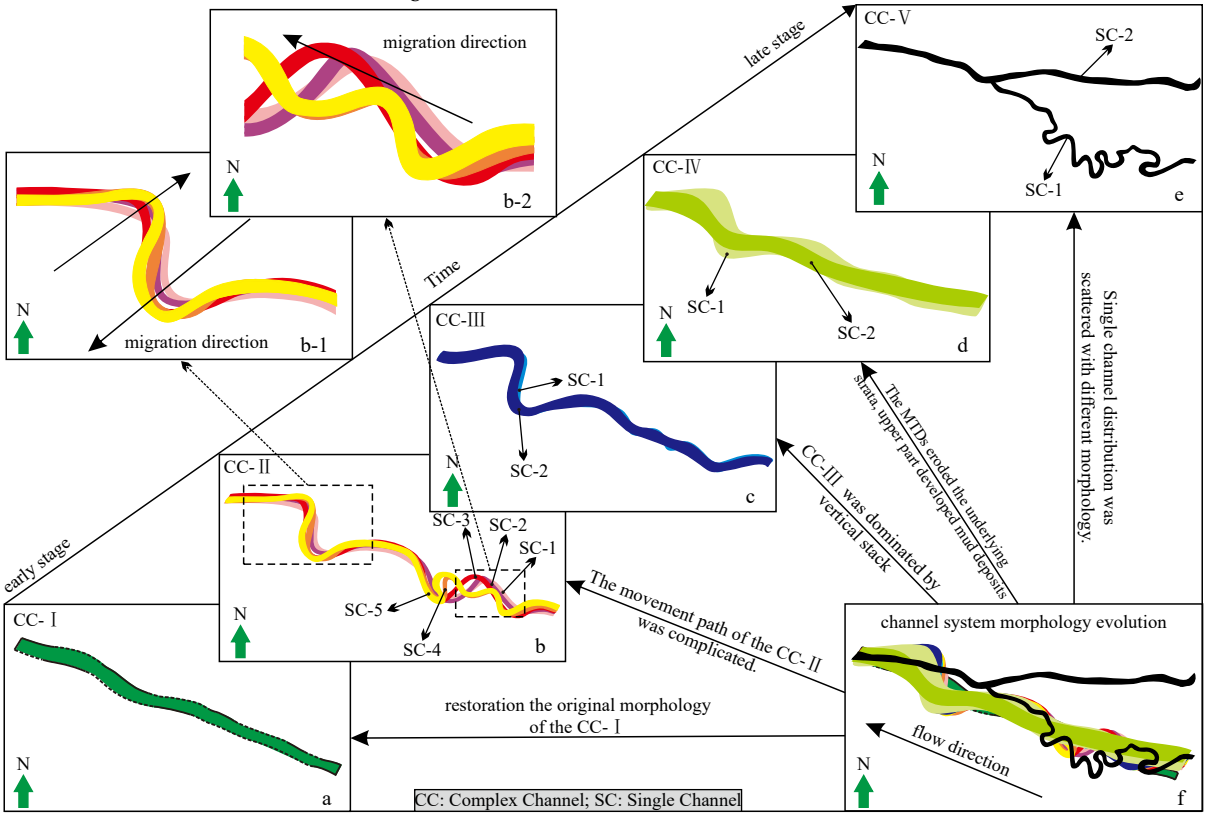

Fig. 9. Schematic diagram of the morphology evolution of each composite channel in the channel system. a. The plane morphology of CC- Ⅰ; the dotted line shows the eroded part of the channel, and the solid line indicates the current residual part of the channel. b. The most complex plane morphology changes in CC- Ⅱ and identifies two types of channel migration: lateral migration (b-1) and downstream migration (b-2). c. The plane morphology of CC-Ⅲ gradually changes from high sinuous to low sinuous. d. CC-Ⅳ shows a relatively straight plane morphology. e. CC- Ⅴ includes a number of single channels with different plane morphologies and disorderly distributions. f. The plane morphology change process of each composite channel in the channel system.

CC-Ⅴ developed multiple single channels and identified multiple different morphological channels in the variance attribute map, in which two single channels with relatively clear morphology were identified: single channel 1 was in a highly sinuous plane morphology, and single channel 2 was in a relatively straight plane morphology (Fig. 9e). These single waterways were spatially scattered and partly beyond the limits range of earlier channels, and the movement direction of the channel was different from the first 4 stages (Fig. 8h). The downcutting depth of the channel at this stage is small.

By analyzing the characteristics of the plane morphology changes of the different composite channels, it can be concluded that the target channel system shows complex plane morphological changes in the process of evolution, and its sinuosity increases rapidly and then gradually decreases, which reflects the characteristics of the channel that tend to equilibrium.

5.2 *Sedimentary evolution of the channel system*

Due to the complexity and variability of the sedimentary evolution of the deep-water channels, a single channel sedimentary evolution model cannot be applied to the study of channels in different environments (Mayall et al., 2006). Deptuck et al. (2007) divided the sedimentary evolution process of the channel into two stages: erosion and filling. In the erosion stage, gravity flow eroded the underlying strata to form sedimentary accommodation, while in the filling stage, sediment deposition and aggregation became the main action. However, the erosion and filling of the channel was a gradual and repeated process. Compared with the proposed channel evolution model from Deptuck et al. (2007), the evolution of the target channel system highlights the erosion of the early channel architectures by multiphase gravity flow, leading to early channel deposits being difficult to keep intact, but because of the characteristics of gravity flow intermittent development, the internal structure of the channel system was more complex.

The target channel system went through several complex erosion-filling cycles, which were divided into three sedimentary evolution stages: initial erosion-filling, later erosion-filling (multistage), and channel abandonment (Fig. 10). Clarifying the evolution process of the channel system can help us understand the development and overlapping characteristics of the channel sedimentary elements in different evolution stages and then predict the distribution position of the channel sand reservoir to provide some reference for subsequent drilling exploration work and reduce the risk of future drilling work.

The initial erosion-filling stage of the composite channel was characterized by the erosion of the underlying strata and the formation of a concave sedimentary accommodation (Figs 10a–e), which provided topographic conditions for the development of subsequent channels (Deptuck et al., 2007; Li et al., 2019). The gravity flow formed by the initial stage has a large scale and strong energy, which can cause strong erosion of the underlying strata and the channel sidewall, thus leading to the large-scale development of slump deposits.

When the energy of gravity flow decreased, the channel began to be filled with sediment. When the new gravity flow developed, it would cause erosion and damage to the early channel again, forming a new sedimentary accommodation and widening the composite channel (Figs 10b, c, and d). With the increase in the flow distance of the gravity flow, the energy of the gravity flow continued to weaken, and the channel was mainly filled with sediment again. When the HDDs developed on the top of the composite channel, they marked the abandonment of the composite

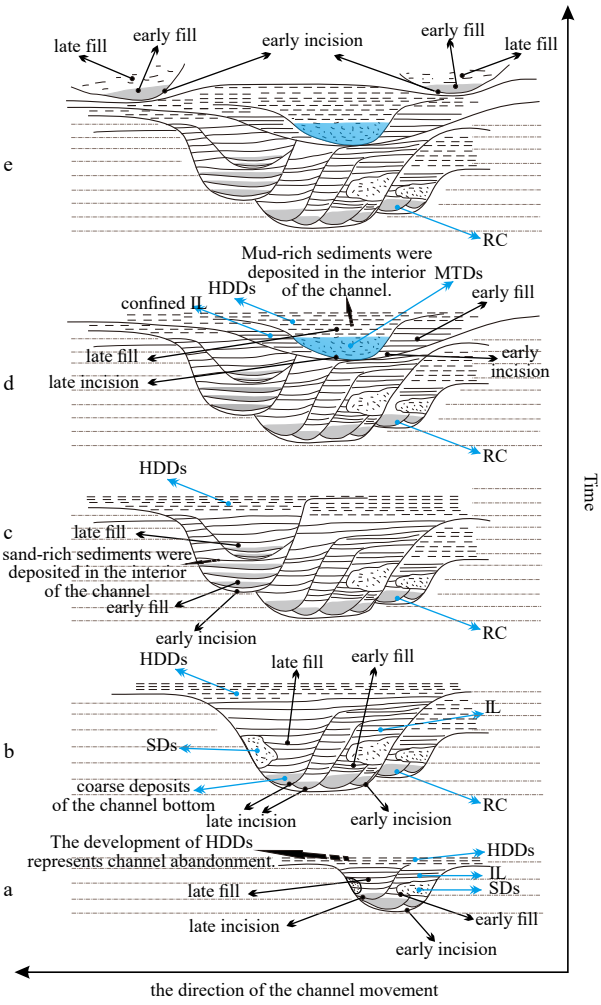

Fig. 10. Sedimentary evolution model of the channel system. The gray filling part of the channel bottom is sand-rich sediment, the blue filling part is mass transport deposits, and the chaotic filling is slump deposits. The blue arrows indicate the sedimentary elements inside the channel, and the black arrows represent the different stages of evolution of the channel.

channel (Figs 10a–e). The deep-water channel was finally filled and covered by the HDDs and then died out, which was the inevitable process of channel evolution (Zhao et al., 2018b). However, there were differences in the scale and energy of gravity flow activities in the composite channels, so the gravity flow in the later erosion-fill stage eroded the early channels many times, thus leading to the continuous increase in the scale of the channel system.

5.3 *Factors affecting the sedimentary evolution and morphology of the channel system*

In the deep-water environment, the evolution of the channel system was controlled by multiple factors (Gee and Gawthorpe, 2006; Wynn et al., 2007). In combination with the geological background, tectonic evolution history, and previous related studies in the study area (Uruski et al., 2002; Bull et al., 2019), we found that the synergy of global climate change and regional tectonic activities controlled the formation of the target channel system, and the morphological changes in the channel system were mostly affected by the self-regulation function of the channel and gravity flow properties.

5.3.1 *Regional tectonic activities and global climate change jointly control the formation of the channel system*

(1) Regional tectonic activities

The regional tectonic activity was an important inducement for the development of the channel system. Uruski and Warburton (2015) proposed that regional plate tectonic activity was the main driving force for the stratigraphic development of the Taranaki Basin in New Zealand. The Taranaki Basin reached the maximum flooding stage at the end of the Oligocene (King and Thrasher, 1996; Strogen et al., 2014), at which time there were few or even missing clastic sediments in New Zealand. The development of the modern plate boundary of New Zealand and the uplift of the New Zealand continent led to the intensification of land erosion and the gradual increase in clastic sediments transported to the deep-water basin (ca. 25 Ma) (Uruski, 2008; Bull et al., 2019; La Marca and Bedle, 2022). These clastic sediments were sufficient to form a new continental shelf and began to advance to the New Caledonian Basin. In the middle Miocene, a large number of terrigenous clastic sediments were transported to the Taranaki Basin, forming several deep-water channels and fans (Uruski, 2008; Baur, 2012; La Marca and Bedle, 2022).

(2) Global climate change

From the Late Eocene to the Early Oligocene, the Tasmania Strait between Antarctica and Australia was opened, and then the Drake Strait between Antarctica and South America was opened, forming the Antarctic circumpolar current. As a result, the heat in the equatorial region was difficult to transport to the south pole, forming a "thermal isolation" environment in the Antarctic region, covering the eastern part of the Antarctic continent with glaciers and triggering a global "ice chamber" event (Zachos et al., 2001; Livermore et al., 2005). The global paleoclimate evolution map showed that from the Late Oligocene to the Middle Miocene, the fluctuation range of $\delta^{18}O$ specific gravity was 1.5%–2.0‰, and since the Middle Miocene, the proportion of global ocean $\delta^{18}O$ continued to increase, indicating that the global climate continued to cool after the Middle Miocene (Fig. 11), which led to global sea-level fall (Haq et al., 1987).

During the Miocene, a global "ice chamber" event and sea-level fall provided sufficient provenance conditions for the development of deep-water sedimentary systems, such as the Lower Congo Basin in West Africa (Yu, 2018; Jia et al., 2019) and the Qiongdongnan Basin in the South China Sea (Xie et al., 2016), where a large number of deep-water channels and fans were developed.

In this study, the development period of the channel system was related to the increase in the global ocean $\delta^{18}O$ proportion in the Middle Miocene, consistent with the fall of global sea level in the Miocene (Fig. 11). The sea-level fall caused by global climate cooling intensified the erosion of the continental shelf area and continental strata in the Taranaki Basin, New Zealand, resulted

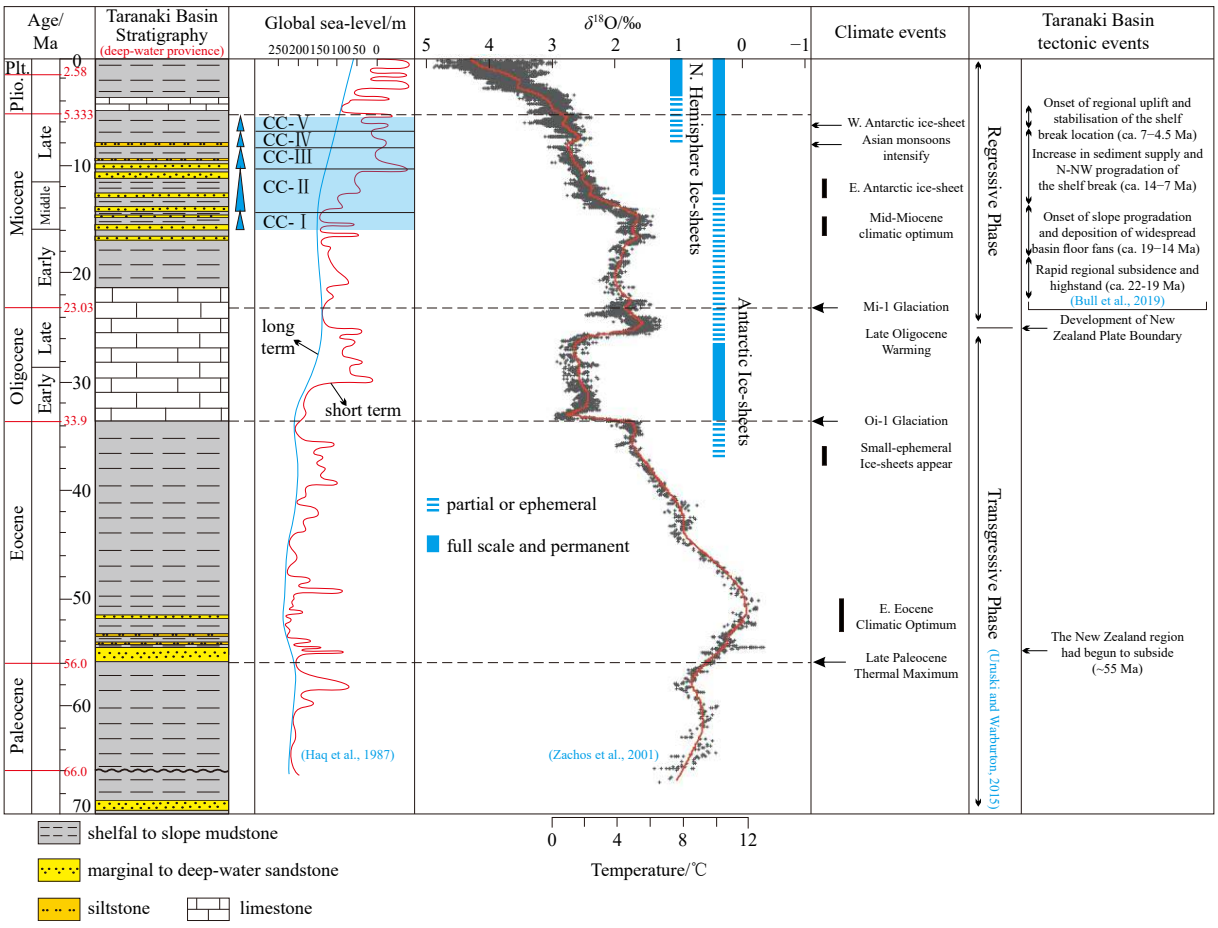

Fig. 11. Stratigraphic characteristics of the deep-water area in the Taranaki Basin, New Zealand (modified after Higgs and King, 2018); Global sea level change curve (modified after Haq et al. (1987)); records of global ocean $\delta^{18}O$ and corresponding climate events (modified after Zachos et al. (2001)); the tectonic events of the Taranaki Basin (modified after Uruski and Warburton (2015) and Bull et al. (2019)).

in a large amount of terrigenous clastic sediments supply to the deep-water basin. Thus, paleoclimate change and the Miocene sea-level fall promoted the development of large-scale channel systems (Uruski, 2008).

5.3.2 *The morphology of the channel system is concurrently controlled by the gravity flow properties and the channel's ability to self-regulate*

An investigation of previous literature showed that the morphological change of the channels is a key part of the study of deep-water deposition, and the sedimentary environment and geological structure conditions in different regions are different, which resulted in different morphological changes in the development of the channels. Peakall et al. (2000) divided the evolution of channels into five stages, with obvious morphological changes in the first three stages: In Stage 1, the channel was relatively straight in morphology, while in Stages 2 and 3, the morphology of the channel gradually became sinuous, and they believed that the possible cause of the channel morphology change was the influence of the submarine topography. Abreu et al. (2003), when exploring lateral accretion packages, proposed that the channels would evolve from the initial straight morphology to the final highly sinuous morphology. However, in the analysis of the plane morphological change of the target channel system, a very interesting phenomenon was observed: the morphology of the channel system underwent relatively straight-highly sinuous-relatively straight cycle changes (Figs 8 and 9), which is different from those observed by Peakall et al. (2000) and Abreu et al. (2003).

Pirmez and Imran (2003) noted that to achieve a smooth channel morphology, the channel could continuously adjust its sinuosity, width, and depth to respond to changes in fluid flow and sediment load. Therefore, the morphological change in the channel system was controlled by the self-regulation function of the channels. Among them, the most prominent performance is CC-Ⅱ, and the abandoned channel formed in Zone 2 reflects the plane morphology changes caused by the self-regulation function of the channel (Fig. 8). The channel system showed an ultrahigh sinuous morphology in Zone 2. Due to the sudden change in the gravity flow in the later stage, a new channel movement path was formed, and the new channel showed a relatively straight morphology (Babonneau et al., 2002; D'Alpaos et al., 2017). The formation of the abandoned channels was a reflection of the self-regulation of channels. An excessively high sinuous degree placed the channels in an unbalanced state.

In CC-Ⅰ, the channel system was relatively straight (Figs 8 and 9), and the movement of the channel in the horizontal direction was restricted, so its morphology change was not obvious (Babonneau et al., 2002). The regional tectonic activities caused the production of a large amount of clastic sediment. In the process of sediment transport to the basin, a gravity flow with strong energy and a large scale was formed (Bull et al., 2019; La Marca and Bedle, 2022). In this stage, the main downcutting caused strong erosion on the lower slope strata. As the sea level gradually fell, clastic sediment formation was controlled in coordination with tectonic activities (Uruski, 2008), producing larger clastic sediments and thus increasing the downcutting depth of the channel. Influenced by the seabed topography shaped by the early channel, the morphology of the channel gradually changed to highly sinuous. Reimchen et al. (2016) proposed using the symmetry of the channel profile to reflect the plane morphology of the channel, and the sinuosity of the channel would increase with the increase in the asymmetry of the channel profile. The Reimchen et al. (2016)'s view was consistent with the morphological change characteristics of CC-Ⅱ, CC-Ⅱ exhibited a highly sinuous plane morphology (Figs 8 and 9). The slow rise in sea level also led to a decrease in sediment supply, the downcutting erosion capacity of the sediment gravity flow was weakened and the aggradation capacity was enhanced, as reflected in the plane morphology, in which the channel gradually began to change from sinuous to relatively straight; that is, CC-Ⅲ and CC-Ⅳ showed these characteristics. Until the final sediment supply was greatly reduced, the erosion capacity of the sediment gravity flow to the underlying stratum was very weak, the resulting negative terrain could not completely limit the gravity flow, and the channel system entered the nonrestrictive environment, forming the characteristics of disorderly channel distribution and different plane morphology; that is, CC-Ⅴ showed these characteristics (Figs 8 and 9).

Therefore, the evolution and morphology of the deep-water channel were controlled by multifactor interaction and joint control. The channel's evolution was primarily influenced by tectonic activity and climate change, with gravity flow properties and the channel's ability to self-regulate acting as auxiliary factors. The Oligocene–Miocene tectonic transformation was the key factor in the formation of a large-scale channel system. The Middle Miocene sea level falls brought on by the global cooling during this time provided sufficient provenance for the development of the channel system, while the gravity flow properties and the channel's ability to self-regulate were the auxiliary factors affecting the morphological characteristics and evolution of the channel system.

6 Conclusions

Three levels of the channel boundary were identified in the seismic profile. According to the four secondary level channel boundaries, the target channel system was divided into five composite channels, and five sedimentary elements were identified in the channel system, namely, channel, slump deposits, levee deposits, mass transport deposits, and hemipelagic drape deposits. Among them, channels included many types, such as remnant channels, lateral migration channels, vertical sand-rich stack channels, vertical mud-rich aggradation channels, single erosion channels, and single aggradation channels. Mass transport deposits and hemipelagic drape deposits can provide good cap rock, while sand-rich infill deposits inside the channel can function as a high-quality hydrocarbon reservoir.

In the process of sedimentary evolution of the channel, the morphology of the composite channel was always changing. The purpose of the morphology change of the deep-water channel was to make the channel itself tend to a balanced and stable state. The plane morphology of CC-Ⅰ was reconstructed and showed a relatively straight morphology. CC-Ⅱ, CC-Ⅲ, and CC-Ⅳ, developed in the restricted environment, underwent a transition from a highly sinuous to relatively straight morphology, while CC-Ⅴ developed in the unrestricted environment showed the characteristics of different plane morphologies and disordered distributions.

The evolution of the channel system was a gradual and repeated erosion-filling process. The evolution of composite channels was divided into three stages: initial erosion-filling, later erosion-filling (multistage), and channel abandonment. The scale of the channel system gradually increased due to the repeatability of the channel erosion-filling process.

The sedimentary evolution of the channel system was affected by many factors. Tectonic activity was the key factor in the

formation of a large-scale channel system. The sea level falls caused by global cooling provided sufficient provenance for the formation of the channel system, while the gravity flow properties and the self-regulation function of the channel assisted in controlling the morphological change and evolution process of the channel.

Data Availability Statements

The data that support the findings of this study are available from the corresponding author upon reasonable request.

Acknowledgements

We are also very grateful to the two reviewers for their helpful comments and text corrections that have significantly improved the paper.

References

Abreu V, Sullivan M, Pirmez C, et al. 2003. Lateral accretion packages (LAPS): an important reservoir element in deep water sinuous channels. Marine and Petroleum Geology, 20(6–8): 631–648, doi: 10.1016/j.marpetgeo.2003.08.003

Alpak F O, Barton M D, Naruk S J. 2013. The impact of fine-scale turbidite channel architecture on deep-water reservoir performance. AAPG Bulletin, 97(2): 251–284, doi: 10.1306/04021211067

Babonneau N, Savoye B, Cremer M, et al. 2002. Morphology and architecture of the present canyon and channel system of the Zaire deep-sea fan. Marine and Petroleum Geology, 19(4): 445–467, doi: 10.1016/S0264-8172(02)00009-0

Babonneau N, Savoye B, Cremer M, et al. 2004. Multiple terraces within the deep incised Zaire Valley (ZaiAngo Project): are they confined levees?. In: Lomas S A, Joseph P, eds. Confined Turbidite Systems. Geological Society Special Publications, 91-114

Babonneau N, Savoye B, Cremer M, et al. 2010. Sedimentary architecture in meanders of a submarine channel: detailed study of the present Congo turbidite channel (Zaiango Project). Journal of Sedimentary Research, 80(10): 852–866, doi: 10.2110/jsr.2010.078

Baur J R. 2012. Regional seismic attribute analysis and Tectonostratigraphy of offshore south-western Taranaki Basin, New Zealand [dissertation]. Wellington: Victoria University of Wellington, 373

Bull S, Nicol A, Strogen D, et al. 2019. Tectonic controls on Miocene sedimentation in the Southern Taranaki Basin and implications for New Zealand plate boundary deformation. Basin Research, 31(2): 253–273, doi: 10.1111/bre.12319

Chima K I, Do Couto D, Leroux E, et al. 2019. Seismic stratigraphy and depositional architecture of Neogene intraslope basins, offshore western Niger Delta. Marine and Petroleum Geology, 109: 449–468, doi: 10.1016/j.marpetgeo.2019.06.030

Clark J D, Pickering K T. 1996. Architectural elements and growth patterns of submarine channels: application to hydrocarbon exploration. AAPG Bulletin, 80(2): 194–220

Collot J, Herzer R, Lafoy Y, et al. 2009. Mesozoic history of the Fairway-Aotea basin: implications for the early stages of Gondwana fragmentation. Geochemistry, Geophysics, Geosystems, 10(12): Q12019

D'Alpaos A, Ghinassi M, Finotello A, et al. 2017. Tidal meander migration and dynamics: a case study from the Venice Lagoon. Marine and Petroleum Geology, 87: 80–90, doi: 10.1016/j.marpetgeo.2017.04.012

Deptuck M E, Sylvester Z, Pirmez C, et al. 2007. Migration-aggradation history and 3-D seismic geomorphology of submarine channels in the pleistocene benin-major canyon, western Niger delta slope. Marine and Petroleum Geology, 24(6–9): 406–433, doi: 10.1016/j.marpetgeo.2007.01.005

Eschard R, Albouy E, Deschamps R, et al. 2003. Downstream evolution of turbiditic channel complexes in the Pab Range outcrops (Maastrichtian, Pakistan). Marine and Petroleum Geology, 20(6–8): 691–710, doi: 10.1016/j.marpetgeo.2003.02.004

Fonnesu M, Palermo D, Galbiati M, et al. 2020. A new world-class deep-water play-type, deposited by the syndepositional interaction of turbidity flows and bottom currents: The giant Eocene Coral Field in northern Mozambique. Marine and Petroleum Geology, 111: 179–201, doi: 10.1016/j.marpetgeo.2019.07.047

Gamboa D, Alves T M. 2015. Spatial and dimensional relationships of submarine slope architectural elements: a seismic-scale analysis from the Espírito Santo Basin (SE Brazil). Marine and Petroleum Geology, 64: 43–57, doi: 10.1016/j.marpetgeo.2015.02.035

Gee M J R, Gawthorpe R L. 2006. Submarine channels controlled by salt tectonics: examples from 3D seismic data offshore Angola. Marine and Petroleum Geology, 23(4): 443–458, doi: 10.1016/j.marpetgeo.2006.01.002

Gong Chenglin, Wang Yingmin, Zhu Weilin, et al. 2013. Upper Miocene to Quaternary unidirectionally migrating deep-water channels in the Pearl River Mouth Basin, northern South China Sea. AAPG Bulletin, 97(2): 285–308, doi: 10.1306/07121211159

Haq B U, Hardenbol J, Vail P R. 1987. Chronology of fluctuating sea levels since the Triassic. Science, 235(4793): 1156–1167, doi: 10.1126/science.235.4793.1156

Higgs K E, Arnot M J, Browne G H, et al. 2010. Reservoir potential of Late Cretaceous terrestrial to shallow marine sandstones, Taranaki Basin, New Zealand. Marine and Petroleum Geology, 27(9): 1849–1871, doi: 10.1016/j.marpetgeo.2010.08.002

Higgs K E, King P R. 2018. Sandstone provenance and sediment dispersal in a complex tectonic setting: Taranaki Basin, New Zealand. Sedimentary Geology, 372: 112–139, doi: 10.1016/j.sedgeo.2018.05.004

Jia Jianzhong, Kang Hongquan, Liu Xiaolong, et al. 2019. Climate events and their bearing on turbidite channels of the Congo Fan. Marine Geology Frontiers (in Chinese), 35(5): 2–10

King P R. 2000. Tectonic reconstructions of New Zealand: 40 Ma to the Present. New Zealand Journal of Geology and Geophysics, 43(4): 611–638, doi: 10.1080/00288306.2000.9514913

King P R, Thrasher G P. 1992. Post-Eocene development of the Taranaki Basin, New Zealand: Convergent overprint of a passive margin. In: Watkins J S, Feng Zhiqiang, McMillen K J, eds. Geology and Geophysics of Continental Margins. Tulsa: American Association of Petroleum Geologists, 93–118

King P R, Thrasher G P. 1996. Cretaceous-cenozoic Geology and Petroleum Systems of the Taranaki Basin, New Zealand. Lower Hutt: Institute of Geological & Nuclear Sciences Monograph, 243

Kolla V, Posamentier H W, Wood L J. 2007. Deep-water and fluvial sinuous channels—Characteristics, similarities and dissimilarities, and modes of formation. Marine and Petroleum Geology, 24(6–9): 388–405, doi: 10.1016/j.marpetgeo.2007.01.007

La Marca K, Bedle H. 2022. Deepwater seismic facies and architectural element interpretation aided with unsupervised machine learning techniques: Taranaki Basin, New Zealand. Marine and Petroleum Geology, 136: 105427, doi: 10.1016/j.marpetgeo.2021.105427

La Marca Molina K, Bedle H, Tellez J. 2020. Seismic attributes and analogs to characterize a large fold in the Taranaki Basin. Interpretation, 8(4): SR27–SR31, doi: 10.1190/INT-2020-0018.1

Li Chao, Chen Guojun, Shen Huailei, et al. 2013. Depositional filling and reservoir distribution patterns of the central canyon in Qiongdongnan Basin. Acta Petrolei Sinica (in Chinese), 34(S2): 74–82

Li Pan, Kneller B, Hansen L. 2021. Anatomy of a gas-bearing submarine channel-lobe system on a topographically complex slope (offshore Nile Delta, Egypt). Marine Geology, 437: 106496, doi: 10.1016/j.margeo.2021.106496

Li Quan, Wu Wei, Kang Hongquan, et al. 2019. Characteristics and controlling factors of deep-water channel sedimentation in Lower Congo Basin, West Africa. Oil & Gas Geology (in Chinese), 40(4): 917–929

Li Quan, Wu Wei, Liang Jianshe, et al. 2020. Deep-water channels in the Lower Congo Basin: Evolution of the geomorphology and depositional environment during the Miocene. Marine and Petroleum Geology, 115: 104260, doi: 10.1016/j.marpetgeo.2020.

104260
Li Quan, Yu Shui, Wu Wei, et al. 2017. Detection of a deep-water channel in 3D seismic data using the sweetness attribute and seismic geomorphology: a case study from the Taranaki Basin, New Zealand. New Zealand Journal of Geology and Geophysics, 60(3): 199–208, doi: 10.1080/00288306.2017.1307230
Livermore R, Nankivell A, Eagles G, et al. 2005. Paleogene opening of Drake Passage. Earth and Planetary Science Letters, 236(1–2): 459–470, doi: 10.1016/j.epsl.2005.03.027
Mayall M, Jones E, Casey M. 2006. Turbidite channel reservoirs—Key elements in facies prediction and effective development. Marine and Petroleum Geology, 23(8): 821–841, doi: 10.1016/j.marpetgeo.2006.08.001
Mayall M, Lonergan L, Bowman A, et al. 2010. The response of turbidite slope channels to growth-induced seabed topography. AAPG Bulletin, 94(7): 1011–1030, doi: 10.1306/01051009117
Moscardelli L, Wood L. 2008. New classification system for mass transport complexes in offshore Trinidad. Basin Research, 20(1): 73–98, doi: 10.1111/j.1365-2117.2007.00340.x
Muir R J, Bradshaw J D, Weaver S D, et al. 2000. The influence of basement structure on the evolution of the Taranaki Basin, New Zealand. Journal of the Geological Society, 157(6): 1179–1185, doi: 10.1144/jgs.157.6.1179
Nwoko J, Kane I, Huuse M. 2020. Mass transport deposit (MTD) relief as a control on post-MTD sedimentation: Insights from the Taranaki Basin, offshore New Zealand. Marine and Petroleum Geology, 120: 104489, doi: 10.1016/j.marpetgeo.2020.104489
Panpichityota N, Morley C K, Ghosh J. 2018. Link between growth faulting and initiation of a mass transport deposit in the northern Taranaki Basin, New Zealand. Basin Research, 30(2): 237–248, doi: 10.1111/bre.12251
Peakall J, McCaffrey B, Kneller B. 2000. A process model for the evolution, morphology, and architecture of sinuous submarine channels. Journal of Sedimentary Research, 70(3): 434–448, doi: 10.1306/2DC4091C-0E47-11D7-8643000102C1865D
Pirmez C, Imran J. 2003. Reconstruction of turbidity currents in Amazon Channel. Marine and Petroleum Geology, 20(6–8): 823–849, doi: 10.1016/j.marpetgeo.2003.03.005
Posamentier H W. 2003. Depositional elements associated with a basin floor channel-levee system: case study from the Gulf of Mexico. Marine and Petroleum Geology, 20(6–8): 677–690, doi: 10.1016/j.marpetgeo.2003.01.002
Prather B E. 2003. Controls on reservoir distribution, architecture and stratigraphic trapping in slope settings. Marine and Petroleum Geology, 20(6–8): 529–545, doi: 10.1016/j.marpetgeo.2003.03.009
Qi Kun, Gong Chenglin, Fauquembergue K, et al. 2022. Did eustatic sea-level control deep-water systems at Milankovitch and timescales? An answer from Quaternary Pearl River margin. Sedimentary Geology, 439: 106217, doi: 10.1016/j.sedgeo.2022.106217
Qin Yongpeng, Alves T M, Constantine J, et al. 2016. Quantitative seismic geomorphology of a submarine channel system in SE Brazil (Espírito Santo Basin): scale comparison with other submarine channel systems. Marine and Petroleum Geology, 78: 455–473, doi: 10.1016/j.marpetgeo.2016.09.024
Rebesco M, Camerlenghi A, Munari V, et al. 2021. Bottom current-controlled Quaternary sedimentation at the foot of the Malta Escarpment (Ionian Basin, Mediterranean). Marine Geology, 441: 106596, doi: 10.1016/j.margeo.2021.106596
Reimchen A P, Hubbard S M, Stright L, et al. 2016. Using sea-floor morphometrics to constrain stratigraphic models of sinuous submarine channel systems. Marine and Petroleum Geology, 77: 92–115, doi: 10.1016/j.marpetgeo.2016.06.003
Shanmugam G. 2000. 50 years of the turbidite paradigm (1950s–1990s): deep-water processes and facies models—a critical perspective. Marine and Petroleum Geology, 17(2): 285–342, doi: 10.1016/S0264-8172(99)00011-2
Steel R J, Olariu C, Zhang Jinyu, et al. 2020. What is the topset of a shelf-margin prism?. Basin Research, 32(2): 263–278, doi: 10.1111/bre.12394
Strogen D P, Bland K J, Nicol A, et al. 2014. Paleogeography of the Taranaki Basin region during the latest Eocene–Early Miocene and implications for the 'total drowning' of Zealandia. New Zealand Journal of Geology and Geophysics, 57(2): 110–127, doi: 10.1080/00288306.2014.901231
Uruski C I. 2008. Deepwater Taranaki, New Zealand: structural development and petroleum potential. Exploration Geophysics, 39(2): 94–107, doi: 10.1071/EG08013
Uruski C I. 2010. New Zealand's deepwater frontier. Marine and Petroleum Geology, 27(9): 2005–2026, doi: 10.1016/j.marpetgeo.2010.05.010
Uruski C I, Stagpoole V, Isaac M J, et al. 2002. Seismic Interpretation Report—Astrolabe Survey, Taranaki Basin, New Zealand. Institute of Geological & Nuclear Sciences confidential client report 2002/70 Open-file Petroleum Report 3072. Ministry of Commerce
Uruski C I., Warburton J. 2015. Sequence stratigraphy and facies prediction: PEP 38451, Deepwater Taranaki Basin. https://www.researchgate.net/publication/265980985
Wang Guangxu, Wu Wei, Lin Changsong, et al. 2022. Migration rules and depositional model of Quaternary deep-water channel in Taranaki Basin, New Zealand. Journal of China University of Petroleum: Edition of Natural Science (in Chinese), 46(3): 13–24
Wu Wei, Li Quan, Yu Jing, et al. 2018. The central canyon depositional patterns and filling process in east of Lingshui depression, Qiongdongnan basin, northern South China Sea. Geological Journal, 53(6): 3064–3081, doi: 10.1002/gj.3143
Wu Wei, Liu Weiqing, Lin Changsong, et al. 2014. Sedimentary evolution of the lower Zhujiang group continental shelf edge in the north slope of Baiyun Sag, Pearl River mouth basin. Acta Geologica Sinica (in Chinese), 88(9): 1719–1727
Wynn R B, Cronin B T, Peakall J. 2007. Sinuous deep-water channels: genesis, geometry and architecture. Marine and Petroleum Geology, 24(6–9): 341–387, doi: 10.1016/j.marpetgeo.2007.06.001
Xie Qinghui, Deng Hongwen. 2013. Application of strata slicing technique in Miocene Congo Fan. Petroleum Geology and Oilfield Development in Daqing (in Chinese), 32(6): 135–140
Xie Yuhong, Fan Caiwei, Zhou Jiaxiong, et al. 2016. Sedimentary features and controlling factors of the gravity flows in submarine fan of Middle Miocene in the Qiongdongnan Basin. Natural Gas Geoscience (in Chinese), 27(2): 220–228
Yu Shui. 2018. Depositional characteristics and pattern of Miocene deep water gravity flow deposits in Lower Cango Basin, West Africa. China Offshore Oil and Gas (in Chinese), 30(4): 13–19
Zachos J, Pagani M, Sloan L, et al. 2001. Trends, rhythms, and aberrations in global climate 65 Ma to present. Science, 292(5517): 686–693, doi: 10.1126/science.1059412
Zhao Xiaoming, Liu Li, Tan Chengpeng, et al. 2018a. Styles of submarine-channel architecture and its controlling factors: a case study from the Niger Delta Basin slope. Journal of Palaeogeography (in Chinese), 20(5): 825–840
Zhao Xiaoming, Qi Kun, Liu Li, et al. 2018b. Development of a partially-avulsed submarine channel on the Niger Delta continental slope: architecture and controlling factors. Marine and Petroleum Geology, 95: 30–49, doi: 10.1016/j.marpetgeo.2018.04.015
Zucker E, Gvirtzman Z, Steinberg J, et al. 2017. Diversion and morphology of submarine channels in response to regional slopes and localized salt tectonics, Levant Basin. Marine and Petroleum Geology, 81: 98–111, doi: 10.1016/j.marpetgeo.2017.01.002